

Role and mechanism of microRNA-23b-3p in regulating high glucose-induced autophagy and apoptosis of human lens epithelial cells

Liu Wenlan, Wang Li, Yang Yang, Yan Jin

School of Medical Technology, Xi'an Medical University, Xi'an 710021, China

Corresponding author: Wang Li, Email: 63148645@qq.com

[Abstract] Objective To investigate the regulatory effects of microRNA-23b-3p (miR-23b-3p) on the autophagy and apoptosis of human lens epithelial cells induced by high glucose.

Methods Thirty diabetic cataract (DC) patients as DC group and 30 patients with simple cataract as simple cataract group were enrolled in The First Affiliated Hospital of Xi'an Medical University from September 2019 to October 2020. Conventional phacoemulsification and intraocular lens transplantation were performed in both groups. The anterior capsular tissue was collected during the operation. The expression of miR-23b-3p in the anterior lens capsule was detected by real-time fluorescence quantitative PCR (RT-qPCR). Human lens epithelial cell line HLEB3 cells were cultured *in vitro* and divided into normal control group and high-glucose group, which were cultured in normal and high-glucose medium, respectively. The targeting relationship between proto-cadherin 17 (PCDH17) and miR-23b-3p was predicted according to the bioinformatics database, and was verified by the dual-luciferase reporter gene experiment. High glucose-cultured HLEB3 cells were divided into miR-23b-3p mimic group, negative control (NC) mimics group, NC-siRNA group, PCDH17-siRNA group, miR-23b-3p mimics+Vector group, miR-23b-3p mimics+pcDNA-PCDH17 group, and were transfected with corresponding reagents according to grouping. The expression of miR-23b-3p and PCDH17 mRNA was detected by RT-qPCR. The expressions of a mammalian homolog of yeast Atg6/Vps30 (Beclin-1), microtubule-associated protein1 light chain 3 (LC3B), c-Jun N-terminal kinases (JNK), phosphorylated (p-) JNK, c-Jun, p-C-Jun, B-cell lymphoma-2 (Bcl-2) and Bcl-2 associated X protein (Bax) proteins were assayed by western blot. The apoptosis rate was detected by flow cytometry. The study protocol was approved by an Ethics Committee of The First Affiliated Hospital of Xi'an Medical College (No. LSL2019037). Written informed consent was obtained from each patient.

Results The relative expression of miR-23b-3p in the anterior lens capsule of DC group was 0.35 ± 0.15 , which was significantly lower than simple cataract group 1.00 ± 0.09 ($t=44.627$, $P<0.01$). There were significant differences in the relative expression levels of miR-23b-3p, LC3B II/I, Beclin-1, Bcl-2 and Bax proteins among normal control group, high glucose group, high glucose+NC mimics group and high glucose+miR-23b-3p mimics group ($F=21.325$, 28.318 , 17.634 , 15.482 , 22.325 , 26.537 , all at $P<0.01$). Compared with normal control group, the apoptosis rate, LC3B II/I, Beclin-1 and Bax protein expressions in high glucose group were significantly increased, and the Bcl-2 protein expression

was significantly decreased (all at $P<0.05$). Compared with NC mimics group, the apoptosis rate, LC3B II/I, Beclin-1, and Bax protein expressions were significantly decreased and the Bcl-2 protein expression was significantly increased in miR-23b-3p mimics group (all at $P<0.05$). The results of bioinformatics and dual-luciferase reporter gene experiments showed that PCDH17 was a target gene of miR-23b-3p, and the relative expression of PCDH17 mRNA in miR-23b-3p mimics group was significantly lower than that in NC mimics group ($P<0.05$). Compared with NC-siRNA group, the apoptosis rate, LC3B-II/I, Beclin-1 and Bax protein expressions in PCDH17-siRNA group were significantly decreased, and the Bcl-2 protein expression was significantly increased, ($t=9.116$, 12.413 , 5.349 , 3.273 , 8.419 ; all at $P<0.01$). There were significant differences in the relative expression levels of p-JNK/JNK, p-c-Jun/c-Jun, LC3B II/I, Beclin-1 and Bcl-2, Bax proteins in NC mimics group, miR-23b-3p mimics group, miR-23b-3p mimics+Vector group and miR-23b-3p mimics+pcDNA-PCDH17 group ($F=24.724$, 19.319 , 23.418 , 17.562 , 20.263 , 15.249 ; all at $P<0.05$). Compared with the miR-23b-3p mimics+Vector group, The expressions of p-JNK/JNK, p-c-Jun/c-Jun, LC3B II/I, Beclin-1 and Bax were significantly increased, and the expression of Bcl-2 protein was decreased in miR-23b-3p mimics+pcDNA-PCDH17 group (all at $P<0.05$).

Conclusions miR-23b-3p has a protective effect on HLEB3 cells in a high-glucose environment, mainly by targeting PCDH17 to regulate the JNK signaling pathway to inhibit high-glucose-induced autophagy and apoptosis in HLEB3 cells.

[Key words] Autophagy; Apoptosis; Diabetic cataract; MicroRNA-23b-3p; Lens epithelial cells

Fund program: 2019 Scientific Research Project of Education Department of Shaanxi Provincial Government (19JK0756); Natural Science Basic Research Plan in Shaanxi Province of China (2021JM-500)

DOI: 10.3760/cma.j.cn115989-20210309-00154

Diabetes is an endocrine disease that seriously affects human health and its prevalence is increasing worldwide. Diabetes cataract (DC) is a major ocular complication characterized by its onset at an early age and rapid progression in patients with diabetes^{1,2}. The incidence of cataracts in patients with diabetes is two to five times that in patients without diabetes, which is the main cause of visual impairment³. Previous studies have

shown that apoptosis of lens epithelial cells plays an important role in the development of cataract⁴. In addition, human lens cells mainly degrade senescent organelles and proteins to maintain lens transparency through autophagy⁵. Lens epithelial cell apoptosis induced by high glucose levels may be one of the causes of DC formation; however, the exact pathogenesis remains unclear. A microRNA (miRNA) is a noncoding single-stranded RNA with a length of 21–23 nucleotides that can silence gene expression by targeting the 3'-untranslated region (UTR) of mRNA molecules via mRNA degradation or translation inhibition^{6,7}. An increasing number of studies have shown that miRNAs play an important role in the pathogenesis of cataracts, such as congenital cataract, aftercataract, and DC^{8–10}. Although miR-23b-3p has been confirmed to be highly expressed in lens tissue¹¹, it remains unclear whether miR-23b-3p is involved in the pathogenesis of DC. Herein, we aimed to investigate the regulatory effect of miR-23b-3p on autophagy and apoptosis in human lens epithelial cells induced by high glucose levels, which is helpful in providing experimental evidence for the prevention and treatment of DC.

1 Materials and methods

1.1 Materials

1.1.1 Sample and cell source

Thirty eyes from 30 patients with DC (DC group) and 30 eyes from 30 patients with simple cataract (control group) were included from September 2019 to October 2022 at the First Affiliated Hospital of Xi'an Medical University. All patients underwent cataract surgery, and then the anterior capsule tissues of the eyes were collected and stored in a cryopreservation tube with liquid nitrogen. In the DC group, the mean age of patients was 64.1 ± 6.9 (range, 61–81) years, including 19 males and 11 females. In the control group, the mean age of patients was 62.2 ± 9.2 (range, 61–79) years, including 17 males and 13 females. The inclusion criteria were as follows: (1) the patients with DC were diagnosed with type 2 diabetes mellitus, along with fasting blood glucose levels of <7.8 mmol/L before surgery and a 4–7-year course of disease; (2) the patients with simple cataract had no history of diabetes mellitus. The exclusion criteria were as follows: (1) patients with cataract due to reasons other than diabetes; (2) patients with glaucoma, vitreous hemorrhage, and other ocular disorders; (3) patients who ignored medical instructions or had incomplete clinical data; and (4) patients with severe systemic disease. There were no significant differences in gender or age between the two groups (all $P > 0.05$). The study protocol was reviewed and approved by the Ethics Committee of the First Affiliated Hospital of Xi'an Medical University (No. LSL2019037). Each patient and family member was informed of the purpose of the experiment and signed an informed consent form. The human lens epithelial cell line HLEB3 was obtained

from the ATCC Cell Bank of the Chinese Academy of Sciences.

1.1.2 The main reagents and equipment

DMEM medium was purchased from Gibco Company (USA). The Annexin V-FITC/PI Cell Apoptosis Detection Kit was purchased from Sigma (USA). The TRIzol reagent, Lipofectamine™ 2000 transfection reagent, was purchased from Invitrogen (USA). The TaqMan miRNA reverse transcription kit was purchased from Beijing Biolab Technology Co., Ltd. The PrimeScript RT-PCR kit and SYBR Green kit were purchased from Takara Company (Japan). RIPA cracking solution was purchased from Shanghai Biyuntian Company. The BCA protein content determination kit was purchased from Thermo Company (USA). The ECL kit was purchased from Beijing Baierdi Biotechnology Co., Ltd. The rabbit anti-human protocadherin 17 (PCDH17) antibody (HPA026817) was purchased from Sigma (USA). The rabbit anti-human c-Jun N-terminal kinase (JNK) antibody (ab199380), rabbit anti-human phosphorylated (p-)JNK antibody (ab47337), rabbit anti-human c-Jun antibody (ab40766), rabbit anti-human p-c-Jun antibody (ab32385), rabbit anti-human microtubule-associated protein 1 light chain 3 (LC3B) antibody (ab192890), rabbit anti-human mammal homolog of yeast Atg6/Vps30 (Beclin-1) antibody (ab207612), rabbit anti-human B lymphomatoma-2-associated X protein (Bax) antibody (ab32503), rabbit anti-human B lymphoma-2 (Bcl-2) antibody (ab32124), and goat anti-rabbit secondary antibody (ab205718) were purchased from Abcam Company (USA). The double luciferase reporter gene vector pGL3 and double luciferase reporter gene detection kit were purchased from Promega (USA). The miR-23b-3p mimics and negative control (NC) mimics were purchased from BGI (Shenzhen, China). The ultraviolet spectrophotometer was purchased from LabTech (USA). The real-time fluorescent quantitative PCR kit was purchased from Applied Biosystems (USA). The Thermo Varioskan™ LUX multifunction microplate reader and CO2 incubator were purchased from Thermo Fisher Scientific (USA). The inverted ordinary optical microscope was purchased from Japan Olympus Company. The electron microscope was purchased from JEOL (Japan). The flow cytometer was purchased from BD (USA). The gel imaging analysis system was purchased from Bio-Rad (USA).

1.2 Methods

1.2.1 Cell culture and grouping treatment

HLEB3 cells were inoculated into DMEM/F12 medium (10% fetal bovine serum, 1% penicillin, and 1% streptomycin) in a 6-well plate for culture. When the cells reached 80% of fusion, culture medium was discarded and then assigned to the medium containing 5 mmol/L of glucose (control group) and the medium containing 25 mmol/L of glucose (high glucose group)

for 48 hrs at 37 °C in atmosphere of 5% CO₂. The cells in high-glucose-level medium were randomly divided into the miR-23b-3p mimic, NC mimic, NC-siRNA, PCDH17-siRNA, miR-23b-3p mimic+Vector, and miR-23b-3p mimic+pcDNA-PCDH17 groups. Subsequently, the cells were transfected in accordance with the instructions of the Lipofectamine™ 2000 kit and cultured for another 24 h for subsequent experiments.

1.2.2 Evaluation of the relative expression of miR-23b-3p and PCDH17 in each group using real-time fluorescent quantitative PCR

HLEB3 cells and anterior capsule tissues were collected in advance. Total RNAs were isolated using the TRIzol reagent and evaluated quantitatively using an ultraviolet spectrophotometer to determine its concentration and purity. Total RNAs were reverse-transcribed into complementary DNA (cDNA) using the PrimeScript RT-PCR kit in accordance with the manufacturer's protocols. Similarly, miRNAs were reverse-transcribed into cDNA using the TaqMan miRNA kit to detect miR-23b-3p expression. qRT-PCR was performed using the SYBR Green PCR Kit. The primers used were as follows: miR-23b-3p (forward, 5'-GAGCATCACATTGCCAGGG-3'; reverse, 5'-GTGCAGGGTCCGAGGT-3'), U6 (forward, 5'-GCTTCGAGCACATATACTAAAAT-3'; reverse, 5'-CGCTTCGGCAGCAATTTGCGTGTTCAT-3'), PCDH17 (forward, 5'-CTTGCGCATGTTGCCTAT-3'; reverse, 5'-CCATCTGTTGCTGCTTTC-3'), and GAPDH (forward, 5'-TGACTTCAACAGCGACACCCA-3'; reverse, 5'-CACCTGTGTGTGTAGTAGCCAAA-3'). The primers were designed and synthesized by Dalian Takara (China). The PCR reaction volume (25 µL), primer (1 µL), and cDNA (2 µL) were used. The PCR reaction condition included pre-denaturation at 95 °C for 30 s and denaturation at 95 °C for 5 s, annealing, and extension at 60 °C for 30 s, with 40 cycles in total. GAPDH and U6 were used as internal references for mRNA and miRNA, respectively. The relative expression of these genes was analyzed using the 2^{-ΔΔCt} method.

1.2.3 Verification of the relationship between miR-23b-3p and the target gene PCDH17 by the double luciferase reporter gene system

Wild-type (WT) and mutant-type (MUT) PCDH17 3'-UTR containing the miR-23b-3p binding site were cloned into the pGL3 vector to obtain a luciferase reporter vector. HLEB3 cells were grown in 96-well plates at a density of 1×10⁴ cells/mL and divided into the NC mimic and miR-23b-3p mimic groups. Thereafter, WT and MUT PCDH17 cells were co-transfected with miR-23b-3p mimics and NC mimics and grown in a cell incubator for 48 h when the cell density reached 70% of fusion. The luciferase activity was detected using a double luciferase analysis system.

1.2.4 Evaluation of the expressions of JNK, p-JNK, c-Jun, p-c-Jun, LC3B, Beclin-1, Bax, and Bcl-2 in each group by western blot

Proteins were isolated from HLEB3 cells in each group and were supplemented with RIPA lysis buffer. The proteins were quantified using a BCA detection kit, and then the samples (30 µg) were subjected to sodium dodecyl sulfate–polyacrylamide gel electrophoresis and transferred onto a polyvinylidene fluoride (PVDF) membrane. After incubation with 5% nonfat milk for 1 h, the PVDF membrane was incubated overnight with specific antibodies. The primary antibodies against JNK, p-JNK, c-Jun, p-c-Jun, LC3B, Beclin-1, Bax, Bcl-2, and GAPDH (all diluted with 1:1,000) were added to cells, incubated overnight at 4 °C, and rinsed with TBST for three times; then, the corresponding secondary antibody (1:2,000) was added, incubated at 37 °C for 1 h, and rinsed with TBST for three times. An ECL kit was used for color development, a gel imaging analysis system was used for detection, and ImageJ software was used for quantitative analysis of the strip. GAPDH was used as the internal reference to measure the relative expression of each target protein.

1.2.5 Detection of the apoptosis rate of HLEB3 cells by flow cytometry

The collected HLEB3 cells were transfected for 48 h, digested with trypsin, and washed twice with phosphate buffer for the normal control, high glucose, miR-23b-3p mimic, NC mimic, NC-siRNA, and PCDH17-siRNA groups. The cells were grown at a density of 1×10⁵ cells per plate. Then, 195 µL of Annexin V-FITC binding buffer was added to prepare a single cell suspension. Subsequently, the collected cells were incubated at room temperature in the dark for 10 min in a mixture of single cell suspension, 5-µL Annexin V-FITC, and 10-µL PI. Apoptosis was analyzed using flow cytometry.

1.3 Statistical analysis

SPSS 21.0 statistical software was used for statistical analysis. All measurement data were verified to be normally distributed using the W test, with $\bar{x} \pm s$ means. The relative expression of miR-23b-3p and expression of proteins associated with apoptosis and autophagy in each miRNA transfection group, the relative expression of PCDH17 mRNA in the cells of each siRNA transfection group, and the JNK pathway protein, autophagy, and apoptosis proteins in the cells of each co-transfection group were compared using single factor analysis of variance, and the comparison between the two groups was performed using the LSD t-test. A *P* value of <0.05 was used as the level of significance.

2 Results

2.1 Comparison of the relative miR-23b-3p expression of the anterior capsule tissues in the simple cataract and DC groups

The relative expression of miR-23b-3p in the lens tissue of patients in the DC group was 0.35±0.15, which was significantly lower than that of patients in the simple cataract group (1.00±0.09), with a statistically

significant difference ($t=44, P<0.01$) (Figure 1).

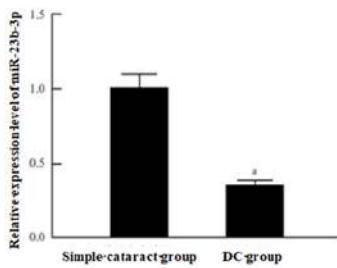


Figure 1 Comparison of the relative expression level of miR-23b-3p in anterior capsular membrane between two groups Compared with simple cataract group, $^aP<0.01$ (Independent samples t test, $n=30$) DC: diabetic cataract; miR: microRNA

2.2 Comparison of the relative miR-23b-3p expression, apoptosis, and autophagy-related proteins in cells transfected with miRNA

There were significant differences in the relative expression levels of miR-23b-3p, LC3B II/I, Beclin-1, Bcl-2, and Bax proteins among the normal control, high glucose, high glucose+NC mimic, and high glucose+miR-23b-3p mimic groups ($F=21.325, P<0.001$; $F=28.318, P=0.002$; $F=17.634, P=0.007$; $F=26.537, P=0.003$; $F=15.482, P=0.001$; and $F=22.325, P<0.001$, respectively). Compared with the normal control group, the apoptosis rate and LC3B II/I, Beclin-1, and Bax protein expressions in the high glucose group significantly increased, whereas the Bcl-2 protein expression significantly decreased (all $P<0.05$). Compared with the NC mimic group, the apoptosis rate and LC3B II/I, Beclin-1, and Bax protein expressions significantly decreased, whereas the Bcl-2 protein expression significantly increased in the miR-23b-3p mimic group (all $P<0.05$) (Figure 2,

Tables 1 and 2).

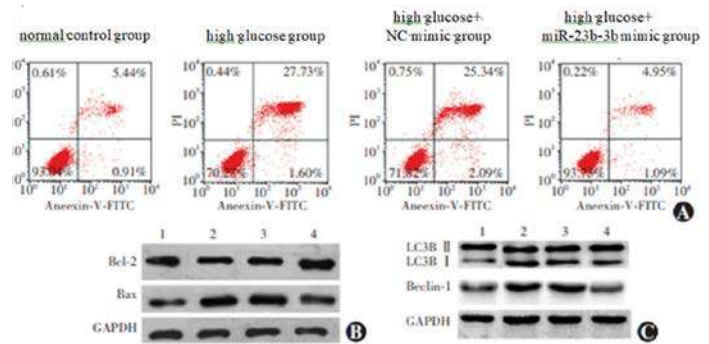


Figure 2 The expressions of apoptosis- and autophagy-related proteins in various groups A: Flow cytometry of apoptosis rate in different groups B: Electrophoretogram of the expression of apoptosis-related proteins C: Electrophoretogram of the expression of autophagy-related proteins 1: normal control group; 2: high glucose group; 3: high glucose+NC mimics group; 4: high glucose+miR-23b-3p mimics group NC: normal control; miR: microRNA; Bcl-2: B-cell lymphoma-2; Bax: Bcl-2 associated X protein; GAPDH: glyceraldehyde-3-phosphate dehydrogenase; LC3B: microtubule-associated protein 1 light chain 3; Beclin-1: a mammalian homolog of yeast Atg6/Vps30

Table 1 Comparison of relative expression level of miR-23b-3p among different groups ($\bar{x}\pm s$)

Group	Sample size	miR-23b-3p expression level
Normal control group	3	1.00±0.11
High glucose group	3	0.39±0.08 ^a
High glucose+NC mimic group	3	0.42±0.07
High glucose+ miR-23b-3p mimic group	3	1.63±0.16 ^b
F		21.325
P		<0.001

Note: Compared with normal control group, $^aP<0.05$; compared with high glucose+NC mimics group, $^bP<0.05$ (One-way ANOVA, LSD- t test) miR: microRNA; NC: negative control

Table 2 Comparison of apoptosis rate and the relative expression levels of autophagy- and apoptosis-related protein among different groups ($\bar{x}\pm s$)

Group	Sample size	LC3B II/I	Beclin-1	Bcl-2	Bax	Apoptotic rate (%)
Normal control group	3	1.02±0.06	1.00±0.05	1.24±0.07	1.01±0.08	4.49±0.69
High glucose group	3	3.12±0.13 ^a	2.89±0.04 ^a	0.53±0.01	3.47±0.22 ^a	19.18±1.13 ^a
High glucose+NC mimic group	3	3.01±0.09	2.82±0.11	0.51±0.03	3.29±0.16	20.61±1.05
High glucose+miR-23b-3p mimic group	3	1.76±0.12 ^b	1.41±0.03 ^b	1.04±0.02	1.54±0.13 ^b	5.83±0.52 ^b
F		28.318	17.634	15.482	2.325	26.537
P		0.002	0.007	0.001	<0.001	0.003

Note: Compared with normal control group, $^aP<0.05$; compared with NC mimic group, $^bP<0.05$ (One-way ANOVA, LSD- t test) LC3B: microtubule-associated protein1 light chain 3; Beclin-1: a mammalian homolog of yeast Atg6/Vps30; Bcl-2: B-cell lymphoma-2; Bax: Bcl-2 associated X protein; NC: negative control; miR: microRNA

2.3 Validation of miR-23b-3p targeting in combination with PCDH17

The bioinformatics database predicted that miR-23b-3p could be targeted directly in combination with the PCDH17 3'-UTR. The luciferase activity of WT-PCDH17 in the miR-23b-3p mimic group was 1.00 ± 0.11 , which was significantly lower than that in the NC mimic group (0.42 ± 0.05) ($t=7.306, P=0.004$). The luciferase activities of MUT-PCDH17 in the miR-23b-3p mimic and NC mimic groups were 1.00 ± 0.09 and 0.98 ± 0.08 respectively, with no significant difference ($t=0.314, P=0.952$). The relative expression of PCDH17 mRNA in the miR-23b-3p mimic group was 0.41 ± 0.04 , which was significantly lower than that of in the NC mimic group (1.00 ± 0.09) ($t=9.483, P=0.001$) (Figure 3).

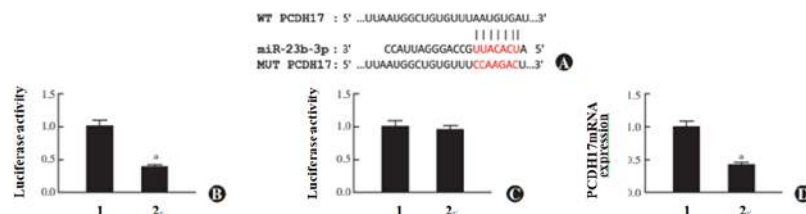


Figure 3 Target binding of miR-23b-3p and PCDH17 A: The binding site of miR-23b-3p targeting to PCDH17 B: Comparison of wild-type luciferase activity between two groups Compared with high glucose+NC mimics group, $^aP<0.05$ (Independent samples t test, $n=3$) C: Comparison of mutant luciferase activity between two groups Compared with high glucose+NC mimics group, $P=0.952$ (Independent samples t test, $n=3$) D: Comparison of the relative expression of PCDH17mRNA among different transfection groups Compared with high glucose+NC mimics group, $^aP<0.05$ (Independent samples t test, $n=3$) 1: high glucose+NC mimics group; 2: high glucose+miR-23b-3p mimics group WT: wild type; PCDH17: protocadherin 17; miR: microRNA; MUT: mutant type

2.4 Comparison of the relative expression of PCDH17 mRNA in cells transfected with siRNA

The relative expressions of PCDH17 mRNA in the normal control, high glucose, NC-siRNA, and PCDH17-siRNA groups were 1.00 ± 0.04 , 3.42 ± 0.16 , 3.35 ± 0.13 , and 1.42 ± 0.09 , respectively, and the overall difference was statistically significant ($F=41$, $P=0.001$). The relative expression of PCDH17 mRNA in the high glucose group was significantly higher than that in the normal control group. The relative expression of PCDH17 mRNA in the PCDH17-siRNA group was significantly lower than that in the NC-siRNA group ($P<0.05$) (Figure 4).

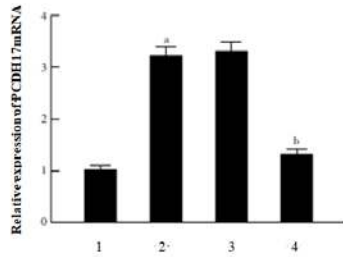


Figure 4 Comparison of relative expression level of PCDH17mRNA among different groups $F=41.183$, $P=0.001$. Compared with normal control group, ^a $P<0.05$; compared with NC-siRNA group, ^b $P<0.05$ (One-way ANOVA, LSD-*t* test, $n=3$) PCDH17: protocadherin 17; NC: negative control 1: normal control group; 2: high glucose group; 3: high glucose+NC-siRNA group; 4:high glucose+PCDH17-siRNA group

2.5 Comparison of the apoptosis rate, apoptosis, and autophagy-related protein expression in cells transfected with siRNA among different groups

Compared with the NC-siRNA group, the apoptosis rate and LC3B-II/I, Beclin-1, and Bax protein expressions in the PCDH17-siRNA group significantly decreased, whereas the Bcl-2 protein expression significantly increased ($t=9.116$, $P=0.001$; $t=12.413$, $P=0.004$; $t=5.349$, $P=0.006$; $t=3.273$, $P=0.001$; and $t=8.419$, $P<0.001$, respectively) (Figure 5 and Table 3).

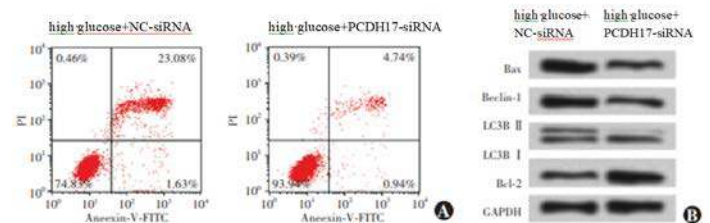


Figure 5 Evaluation of apoptotic rate and expressions of autophagy- and apoptosis-related proteins among different groups A: Flow cytometry of cell apoptosis B: Electrophoretogram of autophagy- and apoptosis-related proteins NC: normal control; PCDH17: protocadherin 17; Bax: Bcl-2 associated X protein; Beclin-1: a mammalian homolog of yeast Atg6/Vps30; LC3B: microtubule-associated protein 1 light chain 3; Bcl-2: B-cell lymphoma-2; GAPDH: glyceraldehyde-3-phosphate dehydrogenase

Table 3 Comparison of apoptosis rate and the relative expression levels of autophagy-related and apoptotic proteins between different siRNA-transfected groups ($\bar{x} \pm s$)

Group	Sample size	LC3B II/I	Beclin-1	Bcl-2	Bax	Apoptotic rate (%)
High glucose+NC-siRNA group	3	1.00 ± 0.09	1.00 ± 0.06	1.00 ± 0.12	1.00 ± 0.10	24.05 ± 1.48
High glucose+PCDH17-siRNA group	3	0.35 ± 0.03	0.39 ± 0.04	3.11 ± 0.28	0.41 ± 0.04	6.31 ± 0.55
<i>t</i>		12.413	5.349	8.419	3.273	9.116
<i>P</i>		0.004	0.006	<0.001	0.001	0.001

Note: (Independent samples *t* test) LC3B: microtubule-associated protein1 light chain 3; Beclin-1: a mammalian homolog of yeast Atg6/Vps30; Bcl-2: B-cell lymphoma-2; Bax: Bcl-2 associated X protein; NC: negative control; PCDH17: protocadherin 17

2.6 Comparison of the JNK pathway proteins, autophagy, and apoptosis proteins in transfected cells among different groups

There were significant differences in the relative expression levels of p-JNK/JNK, p-c-Jun/c-Jun, LC3B II/I, Beclin-1, Bcl-2, and Bax proteins in the NC mimic, miR-23b-3p mimic, miR-23b-3p mimic+vector, and miR-23b-3p mimic+pcDNA-PCDH17 groups ($F=24.724$, $P=0.004$; $F=19.319$, $P=0.008$; $F=23.418$, $P=0.009$; $F=17.562$, $P=0.011$;

$F=20.263$, $P=0.001$; and $F=15.249$; $P=0.005$, respectively). Compared with the NC mimic group, the p-JNK/JNK and p-c-Jun/Jun ratios significantly decreased in the miR-23b-3p mimic group ($P<0.05$). Compared with the miR-23b-3p mimic+Vector group, the expressions of p-JNK/JNK, p-c-Jun/c-Jun, LC3B II/I, Beclin-1, and Bax significantly increased, whereas the expression of Bcl-2 protein decreased in the miR-23b-3p mimic+pcDNA-PCDH17 group (all $P<0.05$) (Figure 6 and Table 4).

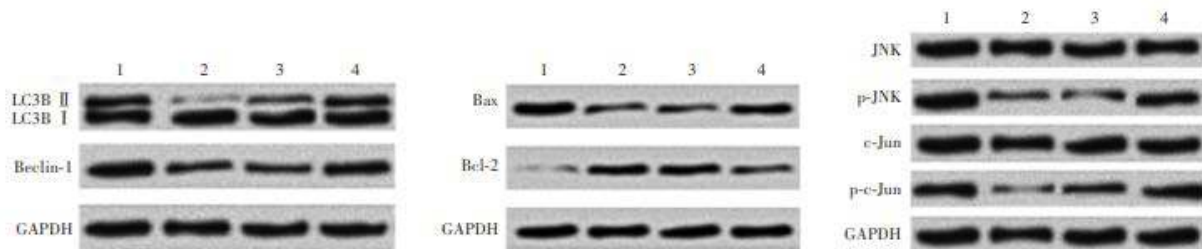


Figure 6 Electrophoretogram of JNK pathway-, autophagy- and apoptosis-related proteins in different co-transfection groups Compared with NC mimics group, the expression bands of p-JNK, p-c-Jun, LC3b II/I, Beclin-1 and Bax proteins were weakened, and the expression bands of Bcl-2 protein were enhanced; compared with miR-23b-3p mimics+vector group, the expression bands of p-JNK, p-c-Jun, LC3b II/I and Bax were stronger, and those of Bcl-2 were weaker LC3B: microtubule-associated protein1 light chain 3; Beclin-1: a mammalian homolog of yeast Atg6/Vps30; GAPDH: glyceraldehyde-3-phosphate dehydrogenase; Bax: Bcl-2 associated X protein; Bcl-2: B-cell lymphoma-2; JNK: c-Jun N-terminal kinases; miR: microRNA; PCDH17: protocadherin 17 1:NC mimic group; 2:miR-23b-3p mimic group; 3: miR-23b-3p mimic+vector group; miR-23b-3pmimic+pcDNA-PCDH17 group

Table 4 Comparison of relative expression level of JNK pathway-, autophagy- and apoptosis-related proteins among different co-transfection groups ($\bar{x}\pm s$)

Group	Sample size	p-JNK/JNK	p-c-Jun/Jun	LC3B II/I	Beclin-1	Bcl-2	Bax
NC mimic group	3	1.01±0.02	1.00±0.06	1.00±0.05	1.00±0.08	1.00±0.02	1.00±0.03
miR-23b-3p mimic group	3	0.43±0.03 ^a	0.31±0.01 ^a	0.33±0.03 ^a	0.39±0.04 ^a	3.14±0.13 ^a	0.31±0.01 ^a
miR-23b-3p mimic+vector group	3	0.41±0.01	0.33±0.02	0.35±0.02	0.40±0.01	3.11±0.08	0.35±0.03
miR-23b-3p mimic+pcDNA-PCDH17 group	3	0.91±0.08 ^b	0.93±0.05 ^b	0.93±0.07 ^b	0.95±0.06 ^b	1.42±0.06 ^b	0.96±0.07 ^b
<i>F</i>		24.724	19.319	23.418	17.562	20.263	15.249
<i>P</i>		0.004	0.008	0.009	0.011	0.001	0.005

Note: Compared with NC mimics group, ^a*P*<0.05; compared with miR-23b-3p mimic+Vector group, ^b*P*<0.05 (One-way ANOVA, LSD-*t* test) JNK: c-Jun N-terminal kinases; LC3B: microtubule-associated protein1 light chain 3; Beclin-1: a mammalian homolog of yeast Atg6/Vps30; NC: negative control; Bcl-2: B-cell lymphoma-2; Bax: Bcl-2 associated X protein; NC: negative control; miR: microRNA; PCDH17: protocadherin 17

3 Discussion

miRNAs are widely involved in apoptosis, cell proliferation, cell differentiation, and stress responses, and their abnormal expression is closely associated with the occurrence of many diseases. Previous studies have reported that miRNAs are abnormally expressed during cataract progression; thus, increasing attention has been paid to the mechanism of DC formation¹²⁻¹³. It has been suggested that miR-23b-3p plays an important role in a variety of tissues and cells, which may inhibit the proliferation and invasion of osteosarcoma cells and promote cell apoptosis by downregulating SIX1¹⁴. Moreover, miR-23b-3p promotes matrix degradation to activate p38 MAPK in chondrocytes of patients with osteoarthritis by regulating HS6ST2¹⁵. miR-23b inhibits neuroinflammation by targeting inositol phosphate kinase and plays a protective role in patients with cerebral hemorrhage¹⁶. In addition, Zhao et al. found that miR-23b-3p regulates cell metabolism induced by high glucose levels in diabetic retinopathy through the SIRT1-dependent signaling pathway¹⁷. CircZNF292 can regulate oxidative stress and lens epithelial cell apoptosis through sponge adsorption of miR-23b-3p in the anterior capsule tissue of patients with age-related cataract¹⁸. Currently, the function and mechanism of miR-23b-3p in DC remain unclear. In this study, HLEB3 cells were cultured in high-glucose-level medium as DC models to investigate the mechanism of action of miR-23b-3p in DC.

Functional changes in lens epithelial cells are considered to be the basis of cataracts at the cellular level. Recent studies have shown that apoptosis and autophagy of lens epithelial cells play vital roles in the occurrence and development of cataracts. It has been shown that lens epithelial cell apoptosis may be the initiating factor of DC formation¹⁹⁻²⁰. The autophagy-lysosome pathway is critical for maintaining lens transparency. Several studies have confirmed that autophagy plays a role in the occurrence and development of various types of cataracts²¹⁻²². The microtubule-associated protein 1 light chain 3 subfamily LC3B is an important ubiquitination system involved in autophagy and acts as a standard indicator of the autophagy level. The LC3-II/LC3-I ratio is typically used to evaluate the autophagy. Beclin-1 is mainly involved in the initial stage of autophagy and is an

important marker for evaluating the autophagy levels. Previous studies have shown that high glucose levels can induce autophagy in vascular endothelial cells²³. In the present study, the results showed that the expressions of LC3B, Beclin-1, and Bax increased in lens epithelial cells cultured in high-glucose conditions, whereas the expression of Bcl-2 decreased, accompanied by cell autophagy and apoptosis. PCDH17 belongs to the protocadherin gene family and has been shown to be related to cell apoptosis and autophagy²⁴⁻²⁶. The function of PCDH17 in DC has not been reported previously. Our results showed that the expression of PCDH17 mRNA in HLEB3 cells increased under high-glucose conditions, whereas the levels of cell autophagy and apoptosis significantly decreased after silencing PCDH17 expression, suggesting that PCDH17 plays an important role in DC. However, the protein level of PCDH17 and mechanism of PCDH17 in DC were not detected in this study, which deserve more attention in subsequent studies. In addition, there is a complex interaction between cell autophagy and apoptosis. It has been reported that activation of autophagy could promote the survival of retinal ganglion cells, whereas inhibition of autophagy could reduce the survival of cells in the process of optic nerve degeneration²⁷. The results of this study showed that both cell apoptosis and autophagy changed significantly during the formation of DC. Nevertheless, the relationship between cell autophagy and apoptosis remains unknown and requires further investigation.

We also explored the potential effect of miR-23b-3p on the JNK signaling pathway in HLEB3 cells induced by high glucose levels. JNK is a member of the mitogen-activated protein kinase family, which can bind to the transcriptional activation domain of phosphorylated c-Jun and plays a crucial role in regulating cellular inflammatory response and cell apoptosis and autophagy²⁸⁻²⁹. Moreover, miR-23b-3p overexpression significantly reduced the p-JNK/JNK and p-c-Jun/Jun ratios, whereas PCDH17 overexpression could reverse this effect, suggesting that miR-23b-3p inhibited the activation of the JNK signaling pathway by regulating PCDH17 in high-glucose-level-induced HLEB3 cells.

In conclusion, miR-23b-3p inhibits the JNK pathway and promotes autophagy and apoptosis in HLEB3 cells

induced by high glucose levels by targeting PCDH17. Our results provide new insights into the molecular mechanisms underlying the occurrence and development of DC. Moreover, it provides the experimental basis of miR-23b-3p as a target for DC therapy.

Conflict of interest None declared

Author contributions Liu WL: Study design and implementation, manuscript writing and revision; Wang L: Study design, data analysis, manuscript review; Yang Y: Study implementation, data collection, data analysis, manuscript revision; Yang J: Data collection, data analysis, manuscript revision.

References

- [1] Peterson SR, Silva PA, Murtha TJ, et al. Cataract surgery in patients with diabetes: management strategies[J]. *Semin Ophthalmol*, 2018, 33(1):75-82. DOI: 10.1080/08820538.2017.1353817.
- [2] Gong X, Ren Y, Fang X, et al. Substance P induces sympathetic immune response in the contralateral eye after the first eye cataract surgery in type 2 diabetic patients[J/OL]. *BMC Ophthalmol*, 2020, 20(1):339[2021-05-02]. <http://www.ncbi.nlm.nih.gov/pubmed/32811461>. DOI: 10.1186/s12886-020-01598-4.
- [3] Wang L, Gong R, Keel S, et al. Ten-year incidence of cataract surgery in urban Southern China: the Liwan Eye Study[J]. *Am J Ophthalmol*, 2020, 217:74-80. DOI: 10.1016/j.ajo.2020.03.034.
- [4] Peng J, Zheng TT, Liang Y, et al. p-Coumaric acid protects human lens epithelial cells against oxidative stress-induced apoptosis by MAPK signaling[J/OL]. *Oxid Med Cell Longev*, 2018, 2018:8549052[2021-05-06]. <http://www.ncbi.nlm.nih.gov/pubmed/29849919>. DOI: 10.1155/2018/8549052.
- [5] Sidjanin DJ, Park AK, Ronchetti A, et al. TBC1D20 mediates autophagy as a key regulator of autophagosome maturation[J]. *Autophagy*, 2016, 12(10):1759-1775. DOI: 10.1080/15548627.2016.1199300.
- [6] Saliminejad K, Khorram Khorshid HR, Soleymani Fard S, et al. An overview of microRNAs: biology, functions, therapeutics, and analysis methods[J]. *J Cell Physiol*, 2019, 234(5):5451-5465. DOI: 10.1002/jcp.27486.
- [7] Ali Syeda Z, Langden S, Munkhzul C, et al. Regulatory mechanism of microRNA expression in cancer[J/OL]. *Int J Mol Sci*, 2020, 21(5):1723[2021-05-02]. <http://www.ncbi.nlm.nih.gov/pubmed/32138313>. DOI: 10.3390/ijms21051723.
- [8] Wu CR, Ye M, Qin L, et al. Expression of lens-related microRNAs in transparent infant lenses and congenital cataract[J]. *Int J Ophthalmol*, 2017, 10(3):361-365. DOI: 10.18240/ijo.2017.03.06.
- [9] Li XT, Qin Y, Zhao JY, et al. Inhibitory effects of microRNA-133b on ultraviolet-induced apoptosis of lens epithelial cells and its mechanism[J]. *Chin J Exp Ophthalmol*, 2017, 35(11):977-983. DOI: 10.3760/cma.j.issn.2095-0160.2017.11.005.
- [10] Liu X, Gong Q, Yang L, et al. microRNA-199a-5p regulates epithelial-to-mesenchymal transition in diabetic cataract by targeting SP1 gene[J/OL]. *Mol Med*, 2020, 26(1):122[2021-05-06]. <http://www.ncbi.nlm.nih.gov/pubmed/33276722>. DOI: 10.1186/s10020-020-00250-7.
- [11] Wu C, Lin H, Wang Q, et al. Discrepant expression of microRNAs in transparent and cataractous human lenses[J]. *Invest Ophthalmol Vis Sci*, 2012, 53(7):3906-3912. DOI: 10.1167/iovs.11-9178.
- [12] Zhang L, Wang Y, Li W, et al. MicroRNA-30a regulation of epithelial-mesenchymal transition in diabetic cataracts through targeting SNAI1[J/OL]. *SciRep*, 2017, 7(1):1117[2021-05-06]. <http://www.ncbi.nlm.nih.gov/pubmed/28442786>. DOI: 10.1038/s41598-017-01320-3.
- [13] Zhang L, Cheng R, Huang Y. MiR-30a inhibits BECN1-mediated autophagy in diabetic cataract[J/OL]. *Oncotarget*, 2017, 8(44):77360-77368[2021-05-06]. <http://www.ncbi.nlm.nih.gov/pubmed/29100392>. DOI: 10.18632/oncotarget.2043.
- [14] Liu H, Wei W, Wang X, et al. miR-23b-3p promotes the apoptosis and inhibits the proliferation and invasion of osteosarcoma cells by targeting SIX1[J]. *Mol Med Rep*, 2018, 18(6):5683-5692. DOI: 10.3892/mmr.2018.9611.
- [15] Guo Y, Min Z, Jiang C, et al. Downregulation of HS6ST2 by miR-23b-3p enhances matrix degradation through p38 MAPK pathway in osteoarthritis[J/OL]. *Cell Death Dis*, 2018, 9(6):699[2021-05-06]. <http://pubmed.ncbi.nlm.nih.gov/29899528>. DOI: 10.1038/s41419-018-0729-0.
- [16] Hu L, Zhang H, Wang B, et al. MicroRNA-23b alleviates neuroinflammation and brain injury in intracerebral hemorrhage by targeting inositol polyphosphate multikinase[J/OL]. *Int Immunopharmacol*, 2019, 76:105887[2021-05-10]. <http://pubmed.ncbi.nlm.nih.gov/31536904>. DOI: 10.1016/j.intimp.2019.105887.
- [17] Zhao S, Li T, Li J, et al. miR-23b-3p induces the cellular metabolic memory of high glucose in diabetic retinopathy through a SIRT1-dependent signalling pathway[J]. *Diabetologia*, 2016, 59(3):644-654. DOI: 10.1007/s00125-015-3832-0.
- [18] Liang S, Dou S, Li W, et al. Profiling of circular RNAs in age-related cataract reveals circZNF292 as an antioxidant by sponging miR-23b-3p[J/OL]. *Aging (Albany NY)*, 2020, 12(17):17271-17287[2021-05-10]. <http://www.ncbi.nlm.nih.gov/pubmed/32913142>. DOI: 10.18632/aging.103683.
- [19] Sun Y, Lu CM, Song Z, et al. Expression and regulation of microRNA-29a and microRNA-29c in early diabetic rat cataract formation[J]. *Int J Ophthalmol*, 2016, 9(12):1719-1724. DOI: 10.18240/ijo.2016.12.03.
- [20] Ahn YJ, Kim MS, Chung SK. Calpain and caspase-12 expression in lens epithelial cells of diabetic cataracts[J]. *Am J Ophthalmol*, 2016, 167:31-37. DOI: 10.1016/j.ajo.2016.04.009.
- [21] Li T, Huang Y, Zhou W, et al. Let-7c-3p Regulates autophagy under oxidative stress by targeting ATG3 in lens epithelial

- cells[OL]. *Biomed Res Int*, 2020, 2020:6069390[2021-05-10]. <http://www.ncbi.nlm.nih.gov/pubmed/32258130>. DOI: 10.1155/2020/6069390.
- [22] Ping X, Liang J, Shi K, et al. Rapamycin relieves the cataract caused by ablation of Gja8b through stimulating autophagy in zebrafish[J]. *Autophagy*, 2021, 17(11):3323-3337. DOI: 10.1080/15548627.2021.1872188.
- [23] Zhao X, Su L, He X, et al. Long noncoding RNA CA7-4 promotes autophagy and apoptosis via sponging MIR877-3P and MIR5680 in high glucose-induced vascular endothelial cells[J]. *Autophagy*, 2020, 16(1):70-85. DOI: 10.1080/15548627.2019.1598750.
- [24] Wu JC, Wang FZ, Tsai ML, et al. Se-Allylselenocysteine induces autophagy by modulating the AMPK/mTOR signaling pathway and epigenetic regulation of PCDH17 in human colorectal adenocarcinoma cells[J]. *Mol Nutr Food Res*, 2015, 59(12):2511-2522. DOI: 10.1002/mnfr.201500373.
- [25] Liu S, Lin H, Wang D, et al. PCDH17 increases the sensitivity of colorectal cancer to 5-fluorouracil treatment by inducing apoptosis and autophagic cell death[OL]. *Signal Transduct Target Ther*, 2019, 4:53[2021-05-17]. <http://pubmed.ncbi.nlm.nih.gov/31815010>. DOI: 10.1038/s41392-019-0087-0.
- [26] Feng Y, Xu W, Zhang W, et al. LncRNA DCRF regulates cardiomyocyte autophagy by targeting miR-551b-5p in diabetic cardiomyopathy[J]. *Theranostics*, 2019, 9(15):4558-4566. DOI: 10.7150/thno.31052.
- [27] Russo R, Varano GP, Adornetto A, et al. Rapamycin and fasting sustain autophagy response activated by ischemia/reperfusion injury and promote retinal ganglion cell survival[OL]. *Cell Death Dis*, 2018, 9(10):981[2021-05-17]. <http://www.ncbi.nlm.nih.gov/pubmed/30250019>. DOI: 10.1038/s41419-018-1044-5.
- [28] Chen J, Ye C, Wan C, et al. The roles of c-Jun N-terminal kinase (JNK) in infectious diseases[OL]. *Int J Mol Sci*, 2021, 22(17):9640[2022-08-08]. <http://www.ncbi.nlm.nih.gov/pubmed/34502556>. DOI: 10.3390/ijms22179640.
- [29] Yan M, Ma Q, Ma YL, et al. Effect and relative mechanism of Lycium Barbarum Polysaccharide on LPS-induced inflammatory response within human retinal pigment epithelial cells[J]. *Int Eye Sci*, 2021, 21(3):411-416. DOI: 10.3980/j.issn.1672-5123.2021.3.06.